

New Electron-Deficient Alkene and Alkyne Derivatives of $\text{Ru}_5(\mu_5\text{-C})(\text{CO})_{15}$: The Syntheses and Crystal Structure Analyses of $\text{Ru}_5(\mu_5\text{-C})(\text{CO})_{13}[\text{C}_2\text{H}_2(\text{CO}_2\text{Me})_2]$ and $\text{Ru}_5(\mu_5\text{-C})(\text{CO})_{15}[\text{C}_2(\text{CO}_2\text{Me})_2]$

Ching-Juh Way,¹ Yun Chi,^{1,3} Ipe J. Mavunkal,¹ Sue-Lein Wang,¹ Fen-Ling Liao,¹ Shie-Ming Peng,² and Gene-Hsiang Lee²

Received August 12, 1996

Treatment of carbido cluster $\text{Ru}_5(\mu_5\text{-C})(\text{CO})_{15}$ with Me_3NO in acetonitrile solution followed by addition of dimethyl maleate or dimethyl acetylene dicarboxylate affords new clusters $\text{Ru}_5(\mu_5\text{-C})(\text{CO})_{13}[\text{C}_2\text{H}_2(\text{CO}_2\text{Me})_2]$ (**1**) and $\text{Ru}_5(\mu_5\text{-C})(\text{CO})_{15}[\text{C}_2(\text{CO}_2\text{Me})_2]$ (**2**), respectively. Single crystal X-ray structural studies reveal that both complexes contain a wingtip-bridged butterfly pentametallic skeleton. In complex **1** the maleate fragment is coordinated to one wingtip Ru atom through its carbon-carbon double bond and to the adjacent Ru atom by the formation of two O → Ru dative bonding interactions, while the acetylene dicarboxylate fragment in **2** is best considered as a *cis*-dimetallated alkene, linking one hinge Ru atom and the nearby Ru atom at the bridged position. Crystal data for **1**: space group $P 4_2/n$; $a = 20.199(6)$, $c = 13.941(3)$ Å, $Z = 8$; final $R_F = 0.025$, $R_w = 0.026$ for 3963 reflections with $I > 2\sigma(I)$. Crystal data for **2**: space group $P2_1/n$; $a = 9.634(3)$, $b = 20.062(6)$, $c = 17.372(5)$ Å, $\beta = 90.62(2)^\circ$, $Z = 4$; final $R_F = 0.033$, $R_w = 0.036$ for 4683 reflections with $I > 3\sigma(I)$.

KEY WORDS: Ruthenium carbide; carbonyl; alkyne; alkene; dimethyl maleate; dimethyl acetylene dicarboxylate.

INTRODUCTION

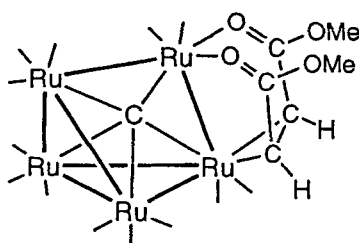
The ruthenium carbido cluster $\text{Ru}_5(\mu_5\text{-C})(\text{CO})_{15}$ was first prepared in trace amount from the reaction of $\text{Ru}_4(\mu\text{-H})_4(\text{CO})_{12}$ with ethylene [1].

¹ Department of Chemistry, National Tsing Hua University, Hsinchu 30043, Taiwan.

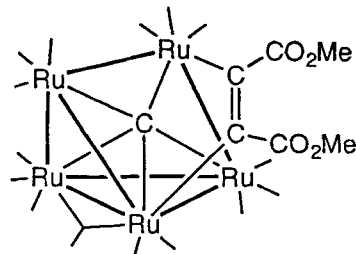
² Department of Chemistry and Instrumentation Center, National Taiwan University, Taipei 10764, Taiwan, Republic of China.

³ To whom all correspondence should be addressed.

Subsequently, an indirect procedure involving the high pressure carbonylation of $\text{Ru}_6(\mu_6\text{-C})(\text{CO})_{17}$ was selected to produce this medium-nuclearity carbido cluster compound in large quantity [2]. Much chemistry of $\text{Ru}_5(\mu_5\text{-C})(\text{CO})_{15}$ has been reported since then. Thus, the further addition of carbon monoxide or weakly coordinated acetonitrile under mild conditions afforded the wingtip-bridged butterfly clusters $\text{Ru}_5(\mu_5\text{-C})(\text{CO})_{16}$ and $\text{Ru}_5(\mu_5\text{-C})(\text{CO})_{15}(\text{NCMe})$, respectively [3]. The addition of $\text{Au}(\text{PPh}_3)\text{Cl}$ to $\text{Ru}_5(\mu_5\text{-C})(\text{CO})_{15}$ formed $\text{Ru}_5(\mu_5\text{-C})(\text{CO})_{14}(\mu\text{-Cl})(\mu\text{-AuPPh}_3)$ which then eliminated one mole of CO to form $\text{Ru}_5(\mu_5\text{-C})(\text{CO})_{13}(\mu\text{-Cl})(\mu\text{-AuPPh}_3)$ where bridging chlorine ligand functions as a three-electron donor [4]. Coordination of H_2S , H_2Se and HSR , $R = \text{Me}$ or Et , led to the formation of the clusters $\text{Ru}_5(\mu_5\text{-C})(\text{CO})_{14}(\mu\text{-H})(\mu\text{-SH})$, $\text{Ru}_5(\mu_5\text{-C})(\text{CO})_{14}(\mu\text{-H})(\mu\text{-SeH})$, and $\text{Ru}_5(\mu_5\text{-C})(\text{CO})_{14}(\mu\text{-H})(\mu\text{-S})$, respectively [5]. In these molecules, the Ru_5 frameworks resemble that of the bridged-butterfly geometry in $\text{Ru}_5(\mu_5\text{-C})(\text{CO})_{15}(\text{NCMe})$ with the hydride associated with the hinge $\text{Ru}\text{-Ru}$ bond and the thiolate group bridging across the hinge and the bridged ruthenium atoms. The nucleophiles, such as with LiMe , NaC_5H_5 and $[\text{PPN}][\text{NO}_2]$, reacted with $\text{Ru}_5(\mu_5\text{-C})(\text{CO})_{15}$ to afford anionic cluster complexes, while upon addition of the aurated cation $[\text{AuPR}_3]^+$, $R = \text{Ph}$ or Et , giving the acyl cluster $\text{Ru}_5(\mu_5\text{-C})(\text{CO})_{14}(\mu\text{-MeCO})(\mu\text{-AuPPh}_3)$, the cyclopentadienyl cluster $\text{CpRu}_5(\mu_5\text{-C})(\text{CO})_{13}(\mu\text{-AuPPh}_3)$ and the nitrosyl cluster $\text{Ru}_5(\mu_5\text{-C})(\text{CO})_{13}(\text{NO})(\mu\text{-AuPEt}_3)$ [6]. In most cases, the reactions are clean and produce only one major product. This novel reactivity pattern has encouraged us to investigate the subsequent reactions of $\text{Ru}_5(\mu_5\text{-C})(\text{CO})_{15}$ with unsaturated hydrocarbons except for the diene molecules, as the latter are known to produce a wide variety of structurally characterized arene clusters [7]. In this paper we describe the reactions of $\text{Ru}_5(\mu_5\text{-C})(\text{CO})_{15}$ with electron-deficient dimethyl maleate and dimethyl acetylene dicarboxylate, and will emphasize on the X-ray structure of the alkene and alkyne derivatives $\text{Ru}_5(\mu_5\text{-C})(\text{CO})_{13}[\text{C}_2\text{H}_2(\text{CO}_2\text{Me})_2]$ (1) and $\text{Ru}_5(\mu_5\text{-C})(\text{CO})_{15}[\text{C}_2(\text{CO}_2\text{Me})_2]$ (2) obtained.



(1)



(2)

EXPERIMENTAL PROCEDURE

General Information and Materials. Infrared spectra were recorded on a Perkin Elmer 2000 FT-IR spectrometer. ^1H and ^{13}C NMR spectra were recorded on a Bruker AM-400 (400.13 MHz) or a AMX-300 (300.6 Mhz) instrument. Chemical shifts are quoted with respect to internal standard tetramethylsilane. Mass spectra were obtained on a JEOL-HX110 spectrometer operating in fast atom bombardment (FAB) mode. All reactions were performed under a nitrogen atmosphere using deoxygenated solvents dried with an appropriate reagent. Reactions were monitored by analytical thin-layer chromatography (5735 Kieselgel 60 F₂₅₄, E. Merck) and the products were separated on commercially available preparative thin-layer chromatographic plates (Kieselgel 60 F₂₅₄, E. Merck). The elemental analyses were performed at the NSC Regional Instrument Center at National Cheng Kung University, Tainan, Taiwan.

Reaction of $\text{Ru}_5(\mu_5\text{-C})(\text{CO})_5$ with Dimethyl Maleate. An acetonitrile solution (10 ml) of freshly sublimed Me_3NO (8.8 mg, 0.12 mmol) was added dropwise into a CH_2Cl_2 solution (25 ml) of $\text{Ru}_5(\mu_5\text{-C})(\text{CO})_{15}$ (50 mg, 0.053 mmol) within 30 min. After the addition of Me_3NO solution was completed, the color of solution faded from red to light red. Dimethyl maleate (60 μl , 0.504 mmol) was added into the flask using a microsyringe. The solvents were removed under vacuum and the oily residue was redissolved into a mixture of CH_2Cl_2 (10 ml) and heptane (30 ml). The heating was continued for 10 min until the color changed to dark red. Then the solvent was removed and the residue was redissolved in the minimum of CH_2Cl_2 and separated by thin-layer chromatography. Development with a 1:2 mixture of dichloromethane and hexane produced an orange band, which was extracted from silica gel to yield 28 mg of $\text{Ru}_5(\mu_5\text{-C})(\text{CO})_{13}[\text{C}_2\text{H}_2(\text{CO}_2\text{Me})_2]$ (**1**, 0.027 mmol, 51 %) after recrystallization.

Spectral data for **1**: MS spectrum (FAB, ^{102}Ru), m/z 1029(M^+). IR(CH_2Cl_2): $\nu(\text{CO})$, 2082 (m), 2046 (vs), 2036 (s), 2023 (s), 1998 (br, m), 1969 (br, m) cm^{-1} ; $\nu(\text{ester-CO})$, 1610 (br, m) cm^{-1} . ^1H NMR (CD_2Cl_2 , 294 K): δ 4.12 (d, ^1H , $J_{\text{H-H}} = 9.4$ Hz), 3.96 (s, 3H), 3.68 (d, ^1H , $J_{\text{H-H}} = 9.4$ Hz), 3.62 (s, 3H). ^{13}C NMR (CD_2Cl_2 , 294 K): δ 463.6 ($\mu_5\text{-C}$), 200.1 (CO), 199.1 (CO), 197.0 (2CO), 196.2 (br, 2CO), 193.1 (CO), 190.9 (CO), 189.0 ($\text{C}=\text{O}_2\text{Me}$), 182.5 ($\text{C}=\text{O}_2\text{Me}$), 55.4 (OCH_3), 55.1 (OCH_3), 40.9 (CH), 37.8 (CH). Elemental analysis for $\text{C}_{20}\text{H}_8\text{O}_{17}\text{Ru}_5$: Calcd.: C, 23.42; H, 0.79. Found: C, 23.25; H, 0.85.

Reaction of $\text{Ru}_5(\mu_5\text{-C})(\text{CO})_{13}[\text{C}_2\text{H}_2(\text{CO}_2\text{Me})_2]$ with CO. To a 50 ml reaction flask, 18 mg of $\text{Ru}_5(\mu_5\text{-C})(\text{CO})_{13}[\text{C}_2\text{H}_2(\text{CO}_2\text{Me})_2]$ (0.017 mmol), 10 ml of CH_2Cl_2 and 15 ml of heptane were added. The resulting

solution was stirred at reflux temperature under a CO atmosphere for 40 min during which time the color changed from orange to dark red slowly. The solvent was removed and the residue was separated by thin-layer chromatography (dichloromethane:hexane = 1:2), affording 8 mg of $\text{Ru}_5(\mu_5\text{-C})(\text{CO})_{15}$ (0.008 mmol, 49 %) as the only isolable product.

Reaction of $\text{Ru}_5(\mu_5\text{-C})(\text{CO})_{15}$ with Dimethyl Acetylene Dicarboxylate. An acetonitrile solution (15 ml) of freshly sublimed Me_3NO (17.6 mg, 0.23 mmol) was added dropwise into a CH_2Cl_2 solution (50 ml) of $\text{Ru}_5(\mu_5\text{-C})(\text{CO})_{15}$ (200 mg, 0.212 mmol) within 30 min. After the addition of Me_3NO solution was completed, the color faded from red to light red. Dimethyl acetylene dicarboxylate (151 μl , 1.23 mmol) was then added into the reaction flask. The mixture was then stirred at room temperature for 20 min. and the color changed to dark red. The solvent was removed under vacuum and the residue was separated by thin-layer chromatography using

Table I. Experimental Data for the X-ray Diffraction Studies^a

Compound	1	2
Empirical formula	$\text{Ru}_5\text{C}_{20}\text{H}_8\text{O}_{17}$	$\text{Ru}_5\text{C}_{22}\text{H}_6\text{O}_{19} \cdot \text{CH}_2\text{Cl}_2$
Crystal system	tetragonal	monoclinic
Space group	$\text{P } 4_2/n$	$\text{P } 2_1/n$
<i>a</i> (Å)	20.199(6)	9.634(3)
<i>b</i> (Å)		20.062(6)
<i>c</i> (Å)	13.941(3)	17.372(5)
β (°)		90.62(2)
Volume (Å ³)	5688(2)	3358(2)
Mol. wt.	1025.62	1164.5
Crystal size, mm.	0.40 × 0.50 × 0.60	0.44 × 0.41 × 0.40
Z	8	4
diffractometer used	Nonius CAD-4	Siemens R3m/V
<i>D_c</i> (/cm ³)	2.395	2.304
<i>F</i> (000)	3872	2208
<i>h, k, l</i> ranges	0 23, 0 23, 0 16	-11 11, 0 23, 0 20
μ (Mo-K α) cm ⁻¹	26.29	24.35
Transmission factors	1.00, 0.924	0.96, 0.82
No. of unique data	4987	5950
No. of observed data	3963 (<i>I</i> > 2 σ (<i>I</i>))	4683 (<i>I</i> > 3 σ (<i>I</i>))
No. of parameters	380	443
Weight modifier	0.00004	0.0006
<i>R_F</i> ; <i>R_w</i> ; G.O.F.	0.025; 0.026; 1.56	0.033; 0.036; 1.34
Maximum Δ/σ ratio	0.006	0.008
Residual electron, e Å ⁻³	0.65/-0.39	1.08/-0.78

^a Features common to all determinations: $\lambda(\text{Mo-K}\alpha) = 0.7107 \text{ \AA}$; minimize function: $\sum (w |F_o - F_c|^2)$, weighting scheme: $w^{-1} = \sigma^2(F_o) + |g| F_o^2$; G.O.F. = $[\sum w |F_o - F_c|^2 / (N_o - N_v)]^{1/2}$ (N_o = number of observations; N_v = number of variables).

Table II. Atomic Coordinates and Equivalent Isotropic Displacement Coefficients for 1

	<i>x</i>	<i>y</i>	<i>z</i>	<i>B</i> (eq) ^a
Ru1	0.054810(20)	0.245366(20)	0.86993(3)	2.645(16)
Ru2	-0.068715(20)	0.200877(21)	0.93198(3)	3.013(17)
Ru3	-0.042721(21)	0.264449(23)	1.11511(3)	3.425(19)
Ru4	0.003463(21)	0.141133(21)	1.08755(3)	3.076(17)
Ru5	0.095042(20)	0.249614(0)	1.06421(3)	2.754(16)
C1	0.0908(3)	0.1636(3)	0.8530(4)	3.82(25)
C2	0.13799(25)	0.28591(25)	0.8338(4)	3.45(23)
C3	-0.0547(3)	0.1163(3)	0.8734(4)	4.5(3)
C4	-0.1585(3)	0.1807(3)	0.9659(4)	5.3(3)
C5	-0.1298(3)	0.2447(3)	1.1567(5)	5.7(3)
C6	-0.0540(3)	0.3574(3)	1.0988(4)	4.6(3)
C7	-0.0177(3)	0.2709(4)	1.2454(4)	7.3(4)
C8	-0.0747(3)	0.0958(3)	1.1287(4)	3.91(25)
C9	0.0479(3)	0.1292(3)	1.2027(4)	5.7(3)
C10	0.0531(3)	0.0695(3)	1.0318(4)	4.4(3)
C11	0.1210(3)	0.3387(3)	1.0380(4)	3.80(24)
C12	0.1213(3)	0.2554(3)	1.1958(4)	3.95(25)
C13	0.17408(24)	0.2027(3)	1.0294(4)	3.64(24)
C14	0.01239(22)	0.22551(23)	1.0008(3)	2.71(20)
C15	-0.0462(3)	0.23849(23)	0.7196(3)	3.39(23)
C16	-0.0976(3)	0.2418(3)	0.7951(3)	3.50(23)
C17	-0.09926(24)	0.2933(3)	0.8664(4)	3.42(22)
C17	-0.09926(24)	0.2933(3)	0.8664(4)	3.42(22)
C18	-0.0506(3)	0.34657(25)	0.8737(3)	3.48(24)
C19	-0.0259(4)	0.2181(4)	0.5554(5)	7.3(4)
C20	-0.0345(4)	0.4615(3)	0.8828(5)	6.2(4)
O1	0.11313(22)	0.11244(19)	0.8387(3)	6.22(23)
O2	0.18844(18)	0.30825(20)	0.8215(3)	5.01(20)
O3	-0.0473(3)	0.06777(20)	0.8319(3)	7.0(3)
O4	-0.21230(21)	0.1698(3)	0.9831(4)	8.9(3)
O5	-0.18049(22)	0.2337(3)	1.1872(4)	9.4(3)
O6	-0.0601(3)	0.41395(21)	1.0982(3)	7.4(3)
O7	-0.0065(3)	0.2763(4)	1.3234(3)	11.9(5)
O8	-0.12084(19)	0.06982(21)	1.1540(3)	5.65(21)
O9	0.0758(3)	0.1192(3)	1.2733(3)	9.6(3)
O10	0.08437(23)	0.02669(20)	1.0052(4)	7.3(3)
O11	0.13330(22)	0.39140(18)	1.0196(3)	5.84(23)
O12	0.13962(22)	0.26048(23)	1.2722(3)	6.57(24)
O13	0.21908(19)	0.17345(22)	1.0083(3)	6.03(23)
O14	0.01341(17)	0.24874(17)	0.72829(22)	3.75(16)
O15	-0.07163(19)	0.22280(19)	0.63579(25)	4.80(19)
O16	0.01044(16)	0.34124(15)	0.87603(23)	3.28(15)
O17	-0.07858(19)	0.40533(17)	0.8781(3)	4.55(18)

^a *B* (eq) is the mean of the principal axes of the thermal ellipsoid.

Table III. Atomic Coordinates and Equivalent Isotropic Displacement Coefficients for 2

	<i>x</i>	<i>y</i>	<i>z</i>	<i>B</i> (eq) ^a
Ru1	0.19203(5)	0.67354(2)	0.16051(3)	2.483(1)
Ru2	0.32883(5)	0.77066(2)	0.06035(3)	2.545(1)
Ru3	0.54051(5)	0.74650(2)	0.17202(3)	2.396(1)
Ru4	0.36057(5)	0.85671(2)	0.18939(3)	2.772(1)
Ru5	0.33189(5)	0.74432(3)	0.28609(3)	2.701(1)
Cl1	0.26120(50)	−0.05445(21)	0.87403(26)	12.539(16)
Cl2	0.16596(66)	0.05164(28)	0.96638(32)	17.037(25)
O1	−0.06617(55)	0.76551(28)	0.16580(40)	5.978(19)
O2	0.06531(58)	0.58101(29)	0.27889(31)	5.593(17)
O3	0.06325(61)	0.58865(28)	0.03185(32)	5.662(17)
O4	0.34772(66)	0.65114(26)	−0.04746(32)	5.499(17)
O5	0.51719(73)	0.85655(32)	−0.04144(37)	6.878(21)
O6	0.05683(66)	0.82402(33)	−0.00604(37)	6.907(20)
O7	0.72089(58)	0.73139(32)	0.02847(32)	5.828(18)
O8	0.73834(60)	0.70879(35)	0.30574(36)	6.438(20)
O9	0.41231(88)	0.97162(32)	0.07748(38)	8.152(26)
O10	0.45974(53)	0.94026(26)	0.32714(32)	5.063(15)
O11	0.06084(58)	0.89722(31)	0.20712(43)	7.139(22)
O12	0.50996(77)	0.80808(32)	0.41156(37)	7.371(22)
O13	0.05353(67)	0.77512(37)	0.35985(39)	7.226(21)
O14	0.37668(71)	0.60733(29)	0.35605(33)	6.388(19)
O15	0.69849(55)	0.87731(26)	0.19067(43)	6.516(20)
O16	0.31097(58)	0.50692(23)	0.19602(29)	4.640(14)
O17	0.37122(53)	0.52231(23)	0.07358(26)	4.165(13)
O18	0.74942(56)	0.61882(29)	0.14522(44)	7.084(22)
O19	0.61003(53)	0.53540(25)	0.16994(39)	5.963(18)
C1	0.02822(70)	0.73222(35)	0.16417(43)	3.810(19)
C2	0.11698(70)	0.61411(33)	0.23460(39)	3.413(17)
C3	0.11169(70)	0.62121(36)	0.07776(41)	3.638(18)
C4	0.34169(73)	0.69548(37)	−0.00787(40)	3.678(18)
C5	0.44637(78)	0.82596(36)	−0.00430(42)	4.028(19)
C6	0.15822(84)	0.80377(37)	0.01756(41)	4.186(20)
C7	0.65501(73)	0.73634(34)	0.08069(41)	3.580(18)
C8	0.66552(76)	0.72150(36)	0.25675(46)	4.052(20)
C9	0.39787(88)	0.92756(38)	0.11784(45)	4.626(22)
C10	0.41868(63)	0.90917(34)	0.27782(40)	3.377(17)
C11	0.17466(78)	0.88272(35)	0.19999(47)	4.358(21)
C12	0.44184(89)	0.78457(39)	0.36578(44)	4.554(21)
C13	0.15937(84)	0.76200(37)	0.33435(41)	4.273(21)
C14	0.35807(80)	0.65814(37)	0.33086(40)	4.014(19)
C15	0.61596(69)	0.83674(33)	0.18263(42)	3.638(18)
C16	0.32610(55)	0.75528(26)	0.17218(31)	2.184(13)
C17	0.37720(62)	0.61540(28)	0.15446(34)	2.571(14)
C18	0.35274(65)	0.54277(30)	0.14630(39)	3.109(16)
C19	0.34695(102)	0.45228(39)	0.05895(51)	5.767(27)
C20	0.50672(65)	0.64120(29)	0.16025(34)	2.829(15)
C21	0.63413(69)	0.59868(33)	0.15712(40)	3.470(18)
C22	0.72555(99)	0.48970(47)	0.16761(70)	8.087(37)
C23	0.13023(142)	−0.00374(70)	0.89266(89)	10.64352

^a *B* (eq) is the mean of the principal axes of the thermal ellipsoid.

Table IV. Selected Bond Distances (Å) and Bond Angles (Deg.) of **1** (esd in Parentheses)

(A) Metal-metal distances			
Ru(1)–Ru(2)	2.7960(9)	Ru(1)–Ru(5)	2.8285(8)
Ru(2)–Ru(3)	2.9056(8)	Ru(2)–Ru(4)	2.8785(8)
Ru(3)–Ru(4)	2.6874(10)	Ru(3)–Ru(5)	2.8873(10)
Ru(4)–Ru(5)	2.8860(10)		
(B) Parameters with the carbide atom			
Ru(1)–C(14)	2.059(5)	Ru(2)–C(14)	1.963(5)
Ru(3)–C(14)	2.097(5)	Ru(4)–C(14)	2.098(5)
Ru(5)–C(14)	1.951(5)		
∠ Ru(2)–C(14)–Ru(5)	177.6(3)	∠ Ru(1)–C(14)–Ru(3)	144.8(2)
∠ Ru(1)–C(14)–Ru(4)	135.2(2)	∠ Ru(3)–C(14)–Ru(4)	79.7(2)
(C) Parameters associated with the alkene ligand			
Ru(1)–O(14)	2.145(3)	Ru(1)–O(16)	2.117(3)
Ru(2)–C(16)	2.161(5)	Ru(2)–C(17)	2.168(5)
C(16)–C(17)	1.437(7)	C(18)–O(16)	1.238(6)
C(18)–O(17)	1.316(6)	C(15)–O(14)	1.228(6)
C(15)–O(15)	1.315(6)		
∠ C(15)–C(16)–C(17)	122.7(4)	∠ C(16)–C(17)–C(18)	124.4(4)
∠ Ru(1)–O(14)–C(15)	118.0(3)	∠ Ru(1)–O(16)–C(18)	119.9(3)

Table V. Selected Bond Distances (Å) and Bond Angles (Deg.) of **2** (esd in Parentheses)

(A) Metal-metal distances			
Ru(1)–Ru(2)	2.934(1)	Ru(1)–Ru(5)	2.920(1)
Ru(2)–Ru(3)	2.841(1)	Ru(2)–Ru(4)	2.843(1)
Ru(3)–Ru(4)	2.828(1)	Ru(3)–Ru(5)	2.838(1)
Ru(4)–Ru(5)	2.827(1)		
(B) Parameters associated with the carbide atom			
Ru(1)–C(16)	2.096(5)	Ru(2)–C(16)	1.967(5)
Ru(3)–C(16)	2.073(5)	Ru(4)–C(16)	2.083(5)
Ru(5)–C(16)	1.99(5)		
∠ Ru(2)–C(16)–Ru(5)	176.4(3)	∠ Ru(1)–C(16)–Ru(3)	123.1(3)
∠ Ru(1)–C(16)–Ru(4)	151.1(3)	∠ Ru(3)–C(16)–Ru(4)	85.7(2)
(C) Parameters associated with the alkyne ligand			
Ru(1)–C(17)	2.135(5)	Ru(3)–C(20)	2.147(6)
C(17)–C(20)	1.354(9)		
∠ C(18)–C(17)–C(20)	122.7(4)	∠ C(17)–C(20)–C(21)	124.4(4)
∠ Ru(1)–C(17)–C(20)	123.9(4)	∠ Ru(3)–C(20)–C(17)	121.5(4)

pure dichloromethane as eluent, affording yellow orange $\text{Ru}_5(\mu_5\text{-C})(\text{CO})_{15}[\text{C}_2(\text{CO}_2\text{Me})_2]$ (**2**, 17.6 mg, 0.016 mmol, 8 %) as the major isolable cluster product. Single crystals suitable for X-ray diffraction study were obtained from a mixture of CH_2Cl_2 and methanol at -20°C .

Spectral data for **2**: MS spectrum (FAB, ^{102}Ru), m/z 1038(M^+). IR(CH_2Cl_2): $\nu(\text{CO})$, 2111 (w), 2081 (s), 2073 (vs), 2068 (s), 2051 (s), 2024 (br, m), 1946 (br, vw) cm^{-1} ; $\nu(\text{ester-CO})$, 1690 (br, w) cm^{-1} . ^1H NMR (CD_2Cl_2 , 294 K): δ 3.52 (s, 3H), 3.48 (s, 3H). (*d*, ^1H , $J_{\text{H-H}} = 9.4$ Hz), 3.96 (s, 3H), ^{13}C NMR (CD_2Cl_2 , 294 K): δ 440.7 ($\mu_5\text{-C}$), 194.9 (2CO), 193.6 (2CO), 192.9 (2CO), 192.6 (CO), 190.9 (3CO), 190.6 (2CO), 189.2 (2CO), 188.3 (CO), 181.7 ($\underline{\text{C}}\text{O}_2\text{Me}$), 171.4 ($\underline{\text{C}}\text{O}_2\text{Me}$), 170.2 ($\underline{\text{C}}_2$), 160.4 ($\underline{\text{C}}_2$), 189.0 ($\underline{\text{C}}\text{O}_2\text{Me}$), 182.5 ($\underline{\text{C}}\text{O}_2\text{Me}$), 51.7 ($\text{O}\underline{\text{C}}\text{H}_3$), 51.5 ($\text{O}\underline{\text{C}}\text{H}_3$). Elemental analysis for $\text{C}_{22}\text{H}_6\text{O}_{19}\text{Ru}_5$: Calcd.: C, 24.48; H, 0.56. Found: C, 24.11; H, 0.72.

X-Ray Crystallography. Diffraction measurements were carried out on a Nonius CAD-4 or a Siemens R3m/V diffractometer. Lattice parameters of **1** were determined from 25 randomly selected high angle reflections with 20 angles in the range 18.50–23.32, whereas the corresponding cell dimensions of complex **2** were determined from 23 reflections with 20 angle in the range of 13.21–27.55. All reflections were corrected for Lorentz, polarization, and absorption effects. All data reduction and refinement were performed using the NRCC-SDP-VAX and Siemens SHELXTL PLUS (VMS) packages. The structures were refined by full-matrix least squares, all nonhydrogen atoms were refined with anisotropic thermal parameters and the hydrogen atoms on organic ligands were calculated in idealized positions and included in the structure factor calculation. The combined data collection and refinement parameters are given in Table I. Atomic positional parameters for complexes **1** and **2** are found in Tables II and III, whereas the selected bond angles and lengths appear in Tables IV and V, respectively.

RESULTS AND DISCUSSION

Synthesis and Characterization of 1. The carbido cluster $\text{Ru}_5(\mu_5\text{-C})(\text{CO})_{15}$ reacts with two equiv. of the oxidative decarbonylation reagent Me_3NO in acetonitrile solution at room temperature to afford an unstable light red complex which is tentatively assigned to have an empirical formula $\text{Ru}_5(\mu_5\text{-C})(\text{CO})_{13}(\text{NCMe})_2$. No attempt is made to isolate and characterize this material. However, upon the addition of excess of dimethyl maleate, it was converted to an orange cluster $\text{Ru}_5(\mu_5\text{-C})(\text{CO})_{13}[\text{C}_2\text{H}_2(\text{CO}_2\text{Me})_2]$ (**1**) in 51 % yield by the incorporation of one dimethyl maleate molecule. The direct reaction of $\text{Ru}_5(\mu_5\text{-C})(\text{CO})_{15}$ with excess dimethyl maleate in dichloromethane containing two equiv. of Me_3NO

also affords the maleate cluster **1**, but the yield is substantially lower. These employed conditions differ from that utilized for the reactions of $\text{Ru}_6(\mu_6\text{-C})(\text{CO})_{17}$ with dienes in producing the arene clusters, where no acetonitrile solvent was added in stabilizing the intermediate [8].

On the contrary, treatment of $\text{Ru}_5(\mu_5\text{-C})(\text{CO})_{15}$ with dimethyl fumarate, in which the CO_2Me functional groups adopt *trans*-disposition at the carbon-carbon double bond, does not produce the corresponding fumarate complex but cluster decomposition. This dramatic diversity in reactivity provides the first indication to the possible involvement of both CO_2Me functional groups in stabilizing the maleate complex **1**.

The maleate cluster **1** is characterized by spectroscopic methods and X-ray diffraction study. The FAB mass spectrum displays a parent molecular ion at m/z 1029, showing the existence of 13 CO ligands and one ligated olefin fragment. The ^1H NMR spectrum is very simple, showing two doublets at δ 4.12 and 3.68 with a coupling constant $^3J_{\text{H-H}} = 9.4$ Hz and two singlet signals at δ 3.96 and 3.62, an indicative of a dimethyl maleate ligand. From these spectroscopic data we can assume that the vacant coordination sites generated by the elimination of two CO ligands is filled by the maleate ligand, which is coordinated to the ruthenium atoms through the carbon-carbon double bond and the oxygen atoms of the carbonyl ligands.

The molecular structure of **1** is shown in Fig. 1 together with the atomic numbering scheme. The selective bond angles and distances are presented in Table IV. The metal core structure is closely related to the "wingtip-bridged butterfly" structure adopted by several analogous pentaruthenium and osmium carbido derivatives [9]. In this molecule, all carbonyl ligands adopt the terminal bonding mode with almost linear Ru-CO angles in the range 173.4 – 179.0° . The Ru-Ru distances are of three types. The shortest is the Ru(hinge)-Ru(hinge) bond (Ru(3)-Ru(4) = $2.6874(10)$ Å), then the Ru(bridge)-Ru(wingtip) bonds (Ru(1)-Ru(2) = $2.7960(9)$ Å and Ru(1)-Ru(5) = $2.8285(8)$ Å) and the longest are the Ru(wingtip)-Ru(hinge) bonds at $2.8860(10)$ – $2.9056(8)$ Å. The Ru(wingtip)-C(14)-Ru(wingtip) angle is nearly linear with angle $177.6(3)^\circ$. The carbide carbon distances to the wingtip ruthenium atoms (Ru(2)-C(14) = $1.963(5)$ Å and Ru(5)-C(14) = $1.951(6)$ Å) are significantly shorter than those to the hinge and bridged ruthenium atoms ($2.059(5)$ Å– $2.098(5)$ Å).

The most striking feature is the bonding of the dimethyl maleate ligand. The alkene portion is coordinated to the Ru(2) atom with distance C(16)-C(17) = $1.438(7)$ Å, which is similar to that observed in the Mo maleate complexes [10]. The carbonyl functional groups are extended across the Ru(1)-Ru(2) bond and coordinated to the adjacent Ru(1) atom with distances Ru(1)-O(14) = $2.145(3)$ Å and Ru(1)-O(16) = $2.117(3)$ Å.

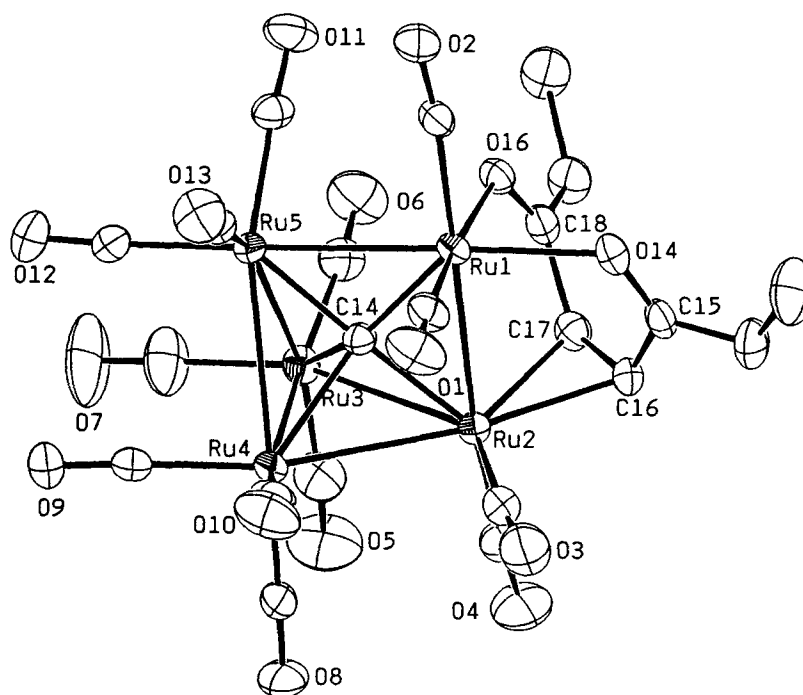


Fig. 1. Molecular structure of $\text{Ru}_5(\mu_5\text{-C})(\text{CO})_{13}[\text{C}_2\text{H}_2(\text{CO}_2\text{Me})_2]$ (**1**) showing the crystallographic labeling scheme with thermal ellipsoids at the 30 % probability level.

These values are typical for the $\text{O} \rightarrow \text{Ru}$ dative bond in triruthenium complexes containing such η^2 -carbonyl group [11], but are slightly shorter than that observed in dinuclear $(\text{C}_5\text{Me}_5)_2\text{Ru}_2(\mu\text{-H})[\text{C}_2\text{H}_2(\text{CO}_2\text{Me})_2][\text{C}_2\text{H}(\text{CO}_2\text{Me})_2]$ (2.23(1) Å) [12] and mononuclear $(\text{Ph}_3\text{P})_3\text{RuH}[\text{CH}=\text{CMe}(\text{CO}_2\text{Bu})]$ (2.246(7) Å) [13], in which the carbonyl oxygen is also coordinated to ruthenium atom. Therefore, the structure of **1** represents the first example in which the dimethyl maleate ligand serves as a six-electron donor through the coordination of its carbon-carbon double bond and both carbonyl fragments.

After understanding the structure of **1**, the mechanism leading to the generation of such novel cluster compound can be envisioned. Basically, formation of **1** may be viewed as an initial coordination by the olefinic portion of the dimethyl maleate, followed by bending of both carbonyl oxygen atoms to the ligand sphere of an adjacent Ru atom. In this case, one oxygen donor replaces the second weakly coordinated acetonitrile ligand, whereas in the formation of the second oxygen to ruthenium atom donor interaction, a Ru-Ru bond is broken. The *cis*-disposition of the carbonyl

groups is important in stabilizing this particular metal framework, as the direct reaction with dimethyl fumarate, which contains two *trans* CO₂Me functional groups, failed to produce the alkene adduct. It seems that the direct linkage with the second carbonyl group and the subsequent cleavage of the Ru–Ru bond are of importance in stabilizing the cluster.

Synthesis and Characterization of 2. Treatment of Ru₅(μ₅-C)(CO)₁₅ with stoichiometric amount of Me₃NO in acetonitrile followed by addition of dimethyl acetylene dicarboxylate results in the formation of pentaruthenium compound Ru₅(μ₅-C)(CO)₁₅[C₂(CO₂Me)₂] (**2**) in 8 % yield as an orange material. The IR spectrum in CH₂Cl₂ solution shows only terminal CO stretches at 2111–1946 cm⁻¹. The ¹H NMR spectrum consists of two methyl resonance signals at δ 3.52 and 3.48, suggesting the presence of one dimethyl acetylene dicarboxylate molecule.

In attempts to explore the possible reaction mechanism, we have varied the conditions by addition of two equivalents of Me₃NO instead.

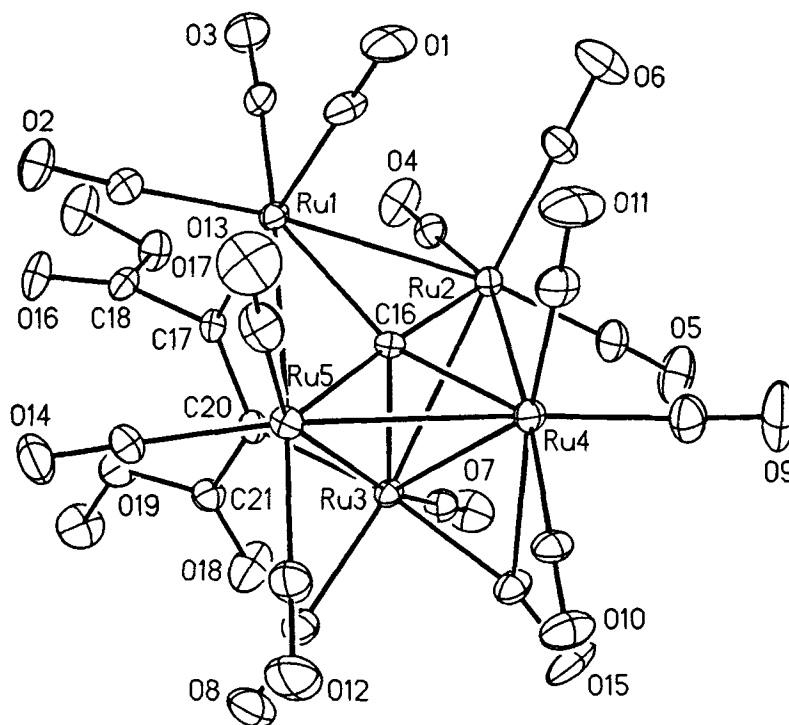


Fig. 2. Perspective drawing of Ru₅(μ₅-C)(CO)₁₅[C₂(CO₂Me)₂] (**2**) showing the crystallographic labeling scheme with thermal ellipsoids at the 30 % probability level.

However, we were unable to isolate compound **2** during this investigation. This observation probably suggests that its formation is the consequence of the coordination of dimethyl acetylene dicarboxylate to the monoacetonitrile cluster complex $\text{Ru}_5(\mu_5\text{-C})(\text{CO})_{14}(\text{NCMe})$ to give an intermediate $\text{Ru}_5(\mu_5\text{-C})(\text{CO})_{14}[\text{C}_2(\text{CO}_2\text{Me})_2]$, followed by recapture of an additional CO ligand in solution. Direct formation of **2** by addition of dimethyl acetylene dicarboxylate across the Ru–Ru bond of $\text{Ru}_5(\mu_5\text{-C})(\text{CO})_{15}$ is precluded because no cluster compound **2** can be isolated in the absence of Me_3NO reagent under similar conditions.

The compound **2** was examined by single-crystal X-ray analysis to determine its molecular structure. The ORTEP diagram is presented in Fig. 2 and the selective distances and angles are given in Table V. The cluster framework is related to that of the previously reported complex **1**, exhibiting the same kind of “wingtip-bridged butterfly” geometry, in which the butterfly fragment is defined the atoms Ru(2), Ru(3), Ru(4), and Ru(5). The alkyne fragment adopts the novel $\mu\text{-}\eta^1, \eta^1$ -bonding mode [14] and spans the nonbonding Ru(1) and Ru(3) atoms. The C(17)–C(20) distance (1.354(9) Å), which falls in the range for a formal carbon–carbon double bond, is slightly longer than the C=C distances (1.27–1.34 Å) seen for the dimetallacyclobutene complexes [15], while the angles ($\angle \text{Ru}(1)\text{--C}(17)\text{--C}(20) = 123.9(4)^\circ$ and $\angle \text{Ru}(3)\text{--C}(20)\text{--C}(17) = 121.6(4)^\circ$) are also consistent with the sp^2 hybridization of the alkene carbons. Thus this alkyne fragment is bound as the *cis*-dimetallated alkene [16]. In addition, all carbonyl ligands adopt a terminal mode, except that the carbonyl ligand C(15)O(15) which bridges the Ru(hinge)–Ru(hinge) bond asymmetrically, $\angle \text{Ru}(3)\text{--C}(15)\text{--O}(15) = 167.6(6)^\circ$. The presence of this bridging CO ligand may be responsible for the slight increase of this Ru(hinge)–Ru(hinge) distance (Ru(3)–Ru(4) = 2.828(1) Å) with respect to the respective hinge Ru–Ru bond in **1**. Moreover, the pattern of the ruthenium–carbide distances is also akin to that of the previous discussed complex **1**, with the distances to the wingtip ruthenium atoms being slightly shorter than those to the hinge and the bridged ruthenium atoms.

SUMMARY AND CONCLUSIONS

The alkene and alkyne derivatives of $\text{Ru}_5(\mu_5\text{-C})(\text{CO})_{15}$, which adopt the wingtip-bridged butterfly geometry, have been synthesized and characterized. Our experimental result suggests that the chemical activation of the parent cluster $\text{Ru}_5(\mu_5\text{-C})(\text{CO})_{15}$ via addition of Me_3NO in the presence of acetonitrile is critical to the successful preparation of these derivatives, although the stoichiometry for the alkyne derivative **2** implies that no prior CO dissociation is required. For the maleate derivative **1**, in addition to the

carbon-carbon double bond, both oxygen atoms of the carbonyl functional groups are linked to a ruthenium atom to compensate for the unsaturation generated by loss of two CO ligands and cleavage of one Ru-Ru bond. The combined interaction from the maleate ligand to the Ru₅ cluster core is still not very effective, as treatment of **1** with CO regenerated the carbonyl cluster Ru₅(μ₅-C)(CO)₁₅ in 49 % yield. In contrast, the dimethyl acetylene dicarboxylate derivative **2**, in which the alkyne is coordinated to the cluster via μ-η¹, η¹-bonding, shows no such carbonyl O → Ru dative interaction due to the unfavorable position of CO₂Me functional groups. Work is currently in progress to investigate the coupling of electron deficient alkenes and alkynes on such pentaruthenium platform. Full details will be presented in forthcoming publications.

SUPPLEMENTARY MATERIALS AVAILABLE

A complete listing of thermal parameters, tables of nonessential bond distances and hydrogen atom coordinates for complexes **1** and **2** are available from the author (Y. C.).

ACKNOWLEDGMENTS

We thank the National Science Council of the Republic of China (Grant No. NSC 85-2113-M007-037CC) for financial support.

REFERENCES

1. C. R. Eady, B. F. G. Johnson, J. Lewis, and T. Matheson (1973). *J. Organomet. Chem.* **57**, C82.
2. (a) B. F. G. Johnson, J. Lewis, S. W. Sankey, K. Wong, M. McPartlin, and W. J. H. Nelson (1980). *J. Organomet. Chem.* **191**, C3; (b) J. N. Nicholls and M. D. Vargas (1989). *Inorg. Synth.* **26**, 280.
3. B. F. G. Johnson, J. Lewis, W. J. H. Nelson, J. N. Nicholls, J. Puga, P. R. Raithby, M. J. Rosales, M. Schröder, and M. D. Vargas (1983). *J. Chem. Soc. Dalton Trans.* 2447.
4. B. F. G. Johnson, J. Lewis, J. N. Nicholls, J. Puga, and K. H. Whitmire (1983). *J. Chem. Soc. Dalton Trans.* 787.
5. A. G. Cowie, B. F. G. Johnson, J. Lewis, J. N. Nicholls, P. R. Raithby, and M. J. Rosales (1983). *J. Chem. Soc. Dalton Trans.* 2311.
6. (a) A. G. Cowie, B. F. G. Johnson, J. Lewis, J. N. Nicholls, P. R. Raithby, and A. G. Swanson (1985). *J. Chem. Soc. Chem. Commun.* 637; (b) K. Henrick, B. F. G. Johnson, J. Lewis, J. Mace, M. McPartlin, and J. Morris (1985). *J. Chem. Soc. Chem. Commun.* 1617.
7. (a) D. Braga, P. Sabatino, P. J. Dyson, A. J. Blake, and B. F. G. Johnson (1994). *J. Chem. Soc. Dalton Trans.* 393; (b) D. Braga, F. Grepioni, P. Sabatino, P. J. Dyson, B. F. G. Johnson, J. Lewis, P. J. Bailey, P. R. Raithby, and D. Stalke (1993). *J. Chem. Soc. Dalton Trans.* 985.

8. P. J. Dyson, B. F. G. Johnson, J. Lewis, M. Martinelli, D. Braga, and F. Grepioni (1993). *J. Am. Chem. Soc.* **115**, 9062.
9. (a) B. F. G. Johnson, J. Lewis, W. J. H. Nelson, J. N. Nicholl, and M. D. Vargas (1983). *J. Organomet. Chem.* **249**, 255; (b) B. F. G. Johnson, J. Lewis, P. R. Raithby, M. J. Rosales, and D. A. Welch (1986). *J. Chem. Soc. Dalton Trans.* 453; (c) B. F. G. Johnson, J. Lewis, W. P. R. Raithby, V. P. Saharan, and W. T. Wong (1992). *J. Organomet. Chem.* **434**, C10.
10. C. H. Lai, C. H. Cheng, W. C. Chou, and S. L. Wang (1993). *Organometallics* **12**, 3418.
11. (a) M. I. Bruce, P. A. Humphrey, H. Miyamae B. W. Skelton, and A. H. White (1992). *J. Organomet. Chem.* **429**, 187; (b) U. Bodensieck, J. Santiago, H. Stoeckli-Evans and G. Süss-Fink (1992). *J. Organomet. Chem.* **433**, 141; (c) D. S. Bohle, A. N. Christensen and P. A. Goodson (1993). *Inorg. Chem.* **32**, 4173.
12. H. Suzuki, H. Omori, D. H. Lee, Y. Yoshida, M. Fukushima, M. Tanaka, and Y. Moro-oka (1994). *Organometallics* **13**, 1129.
13. S. Komiya, T. Ito, M. Cowie, A. Yamamoto, and J. Ibers (1976). *J. Am. Chem. Soc.* **98**, 3874.
14. C. P. Casey, R. S. Carino, R. K. Hayashi, and K. D. Schladetzky (1996). *J. Am. Chem. Soc.* **118**, 1617.
15. (a) J. Holton, M. F. Lappert, R. Pearce, and P. I. Yarrow (1983). *Chem. Rev.* **83**, 135; (b) M. R. Burke and J. Takats (1986). *J. Organomet. Chem.* **302**, C25.
16. K. A. Johnson and W. L. Gladfelter (1991). *J. Am. Chem. Soc.* **113**, 5097.